Published in final edited form as:

Glia. 2016 December ; 64(12): 2247–2262. doi:10.1002/glia.23072.

Cadm3 (Necl-1) interferes with the activation of the PI3 kinase/Akt signaling cascade and inhibits Schwann cell myelination *in vitro*

Ming-Shuo Chen, **Hyosung Kim**, **Léonard Jagot-Lacoussiere**, and **Patrice Maurel**

Rutgers, The State University of New Jersey, Newark, NJ 07102

Abstract

Axo-glial interactions are critical for myelination and the domain organization of myelinated fibers. Cell adhesion molecules belonging to the Cadm family, and in particular Cadm3 (axonal) and its heterophilic binding partner Cadm4 (Schwann cell), mediate these interactions along the internode. Using targeted shRNA-mediated knockdown, we show that the removal of axonal Cadm3 promotes Schwann cell myelination in the *in vitro* DRG neuron/Schwann cell myelinating system. Conversely, over-expressing Cadm3 on the surface of DRG neuron axons results in an almost complete inability by Schwann cells to form myelin segments. Axons of superior cervical ganglion (SCG) neurons, which do not normally support the formation of myelin segments by Schwann cells, express higher levels of Cadm3 compared to DRG neurons. Knocking down Cadm3 in SCG neurons promotes myelination. Finally, the extracellular domain of Cadm3 interferes in a dose-dependent manner with the activation of ErbB3 and of the pro-myelinating PI3K/Akt pathway, but does not interfere with the activation of the Mek/Erk1/2 pathway. While not in direct contradiction, these *in vitro* results shed lights on the apparent lack of phenotype that was reported from *in vivo* studies of Cadm3$^{-/-}$ mice. Our results suggest that Cadm3 may act as a negative regulator of PNS myelination, potentially through the selective regulation of the signaling cascades activated in Schwann cells by axonal contact, and in particular by type III Nrg-1. Further analyses of peripheral nerves in the Cadm$^{-/-}$ mice will be needed to determine the exact role of axonal Cadm3 in PNS myelination.

Keywords

cell adhesion; Cadm3; myelination; Schwann cell; neuregulin

Introduction

Myelination of axons in the peripheral nervous system (PNS) is a complex process that results from the integration of numerous signals by the myelinating Schwann cell. These

Corresponding Author: Patrice Maurel, Rutgers – The State University of New Jersey, Department of Biological Sciences, Boyden Hall room 206, 195 University Ave, Newark NJ 07102 maurep01@andromeda.rutgers.edu.
Léonard Jagot-Lacoussiere present address: INSERM UMRS 1160, Université Denis Diderot, Institut Universitaire d'Hématologie, Hôpital Saint-Louis, Paris, France.

signals originate in multiple domains of the Schwann cell, in particular at the adaxonal (axon-glia) and abaxonal (extracellular matrix-glia) interfaces (Pereira et al. 2012).

Among the molecular mechanisms acting at the axon - Schwann cell interface, signals provided by axon-derived neuregulin-1 (Nrg1) growth factors have been shown to regulate many aspects of Schwann cell development. Studies using knockout strategies have provided compelling evidence that membrane-bound type III Nrg1 is the key isoform required for Schwann cell proliferation and survival (Meyer et al. 1997; Wolpowitz et al. 2000). Type III Nrg1 is also the instructive axonal signal that determines in the PNS whether a Schwann cell ensheathes multiple axons (Remak bundles) or associates in a 1:1 relationship with an axon and forms a myelin sheath (Taveggia et al. 2005). The levels of type III Nrg1 on axons further regulate the extent of myelination by determining the number of lamellae that myelinating Schwann cells will form around axons (Michailov et al. 2004; Taveggia et al. 2005). ErbB2 and ErbB3 (erythroblastic leukemia viral oncogene homologs 2 and 3) are the tyrosine kinase receptors that transduce the Nrg1 signal within Schwann cells (Garratt et al. 2000). The ErbB2/3 complex elicits three major signaling cascades: i) the PI3 kinase/Akt pathway is involved in the regulation of proliferation and survival (Maurel and Salzer 2000), as well as myelin thickness (Cotter et al. 2010; Goebbels et al. 2012); ii) activation of the PLCγ/Ca^{2+}/calcineurin cascade results in the nuclear translocation of NFATc4, which with Sox10 regulates the transcription of Krox20 and Mpz (Kao et al. 2009); iii) activation of the MEK/Erk1/2 cascade, which has been shown to promote Krox20 transcription (He et al. 2010). Interestingly the MEK/Erk1/2 cascade appears to be both pro-myelinating (Newbern et al. 2011) and inhibitory to PNS myelination (Ogata et al. 2004; Syed et al. 2010).

Axons and Schwann cells also interact through several cell adhesion molecules. These interactions are important insofar that they participate in the organization of the specialized domains that are characteristic of myelinated axons (node of Ranvier, paranode, juxtaparanode) and whose structure and molecular composition are crucial to the fast propagation of action potentials by saltatory conduction (Salzer et al. 2008). Nectin-like (Necl) proteins (also referred to as Cadm [cell adhesion molecule] and SynCAM [synaptic cell adhesion molecule]) are type 1 transmembrane cell adhesion molecules (Biederer 2006; Takai et al. 2008). Schwann cells mainly express Cadm4 (Necl-4), while DRG neurons express Cadm3 (Necl-1). Both cell types also express Cadm1 (Necl-2) (Maurel et al. 2007; Spiegel et al. 2007). They promote axon-to-Schwann cell interaction along the internodal domain through heterophilic (Schwann cell Cadm4 and Cadm1 to axonal Cadm3) and homophilic (Cadm1 to Cadm1) binding (Maurel et al. 2007; Spiegel et al. 2007). Schwann cell-specific Cadm4 has been shown to be a key molecule in initiating PNS myelination (Maurel et al. 2007; Spiegel et al. 2007). Indeed, shRNA-mediated knockdown of Cadm4 blocked Schwann cell differentiation and myelination in a Schwann cell/DRG neuron myelinating co-culture system, as was indicated by the absence of myelin proteins and myelin segments (Maurel et al. 2007). The limited expression of transcription factors Oct-6 and Krox-20 indicated that Schwann cells were arrested before progressing to the promyelinating stage (Maurel et al. 2007). Experiments using the addition of the extracellular domains of Cadm4 or Cadm3 to perturb axo-glial interactions at the onset of myelination in the co-culture system similarly resulted in a drastic reduction in myelin segments formation (Spiegel et al. 2007). Electron microscopy analysis showed that

Schwann cells ensheathed but failed to wrap axons (Spiegel et al. 2007). In that respect it is interesting to note that, among the myelination abnormalities that were described in the recent analysis of a Cadm4 knockout mouse, there is a delay in the initiation of PNS myelination (Golan et al. 2013).

The Cadm4 knockout mouse also presents several abnormalities along the axo-glial interface that are indicative that Cadm4 is essential to promote a proper interaction between the axon and the myelinating Schwann cell (Golan et al. 2013). Both Cadm3 and Cadm2 (Necl-3) are binding partners for Cadm4 (Maurel et al. 2007; Thomas et al. 2008). While Cadm2 promotes axo-glial interaction in the central nervous system (CNS) (Pellissier et al. 2007), it is not as clear in the PNS. While it appears to be present in trigeminal neurons (Pellissier et al. 2007), Cadm2 is barely detectable in DRG neurons (Maurel et al. 2007; Spiegel et al. 2007). It also appears to be limited to the DRG neuron bodies and absent from the axons (Maurel et al. 2007). While additional axonal binding partners for Cadm4, as yet uncharacterized, could be upregulated with myelination, the current data strongly suggest that Cadm3, on the axon, is the obligate binding partner for Cadm4 present on the Schwann cell.

Surprisingly, the analyses of two independent Cadm3 knockout mice have shown no detectable defects in PNS myelination (Golan et al. 2013; Park et al. 2008). This could potentially be attributed, in part, to the complexity of *in vivo* systems in which redundancy and functional overlap may obscure the detection of a phenotype. We therefore investigated *in vitro* a potential role for axonal Cadm3 in myelination, using the well-established Schwann cell/DRG neuron myelinating co-culture system that has been central to many key insights in the molecular mechanisms involving axo-glial interactions, domain formations and myelination. An expected outcome of suppressing the expression of Cadm3 in DRG neurons would have been a decrease in myelination by Schwann cells. However we report that the ablation of Cadm3 from DRG neurons results in a 2-fold increase in the number of myelinated segments. Conversely, increased expression of Cadm3 at the surface of DRG neuron axons results in an almost complete inability by Schwann cells to form myelin segments. We show that SCG neurons, which do not normally support (both *in vitro* and *in vivo*) the formation of myelin segments by Schwann cells, express higher levels of Cadm3 compared to DRG neurons. Knocking down Cadm3 expression in SCG neurons promotes myelination. Finally we show that the binding of the extracellular domain of Cadm3 to Schwann cells inhibits activation of the ErbB3/PI3K/Akt signaling cascade by the EGF-like domain of Nrg1β1. These results, obtained *in vitro*, are in contrast to the apparent lack of phenotype *in vivo*. While they point to a regulatory function for axonal Cadm3, to suppress myelination, further detailed studies of the Cadm3 knockout mice will be needed to determine the exact function of Cadm3 in *in vivo* PNS myelination.

Material and Methods

Animals, culture media, antibodies and growth factors

Sprague-Dawley rats were from the colony maintained at the animal facility at Rutgers, The State University of New Jersey, Newark NJ. They were housed and cared for in accordance with an animal protocol approved by Rutgers University Institutional Animal Care and Use

Committee. DMEM and MEM were from Mediatech, neurobasal media, Ham's F12, B27 supplement, N2 supplement, GlutaMAX^{TM}-I and trypsin were from Invitrogen, glucose, Forskolin, 5-fluorodeoxyuridine, uridine and ascorbic acid were from Sigma-Aldrich, FBS was from Atlas Biological, and Matrigel was from Beckton Dickinson. For immunofluorescence staining, primary antibodies included mouse monoclonals to myelin basic protein (MBP) (Covance SMI-94R at 1:300) and HA epitope (Covance HA.11 at 1:500), and the chicken monoclonal to neurofilament M (Covance PCK-593P at 1:3000). For Western blot analyses, primary antibodies included mouse monoclonals to β-actin (Sigma Aldrich A1978 at 1:5000), GFAP (Cell Signaling Technology 3670 at 1:1000), Cadm4 (Necl4, NeuroMab 75-247 at 1:1000), ErbB2 (Thermo Scientific MS-730 at 1:500), ErbB3 (Thermo Scientific MS-201 at 1:500), phospho-Akt (S^{473}; Cell Signaling Technology 4051 at 1:1000), Erk1/2 (Cell Signaling Technology 4696 at 1:1000), mouse polyclonal against the Fc portion of human IgG (Jackson ImmunoResearch 209-005-098 at 1:1000), rabbit polyclonals against phospho-ErbB2 (Tyr^{1248}; Santa Cruz sc-12352-R at 1:500), phospho-ErbB3 (Tyr^{1289}; Cell Signaling Technology 4791 at 1:500), Akt (Cell Signaling Technology 9272 at 1:1000), phospho-Erk1/2 (Thr^{202}/Tyr^{204}; Cell Signaling Technology 9101 at 1:1000), PTPN13 (Santa Cruz sc-15356 at 1:200), neuregulin-1-β1 (Santa Cruz sc-348 at 1:250), TrkA ((Clary et al. 1994) at 1:500), Cadm2 (Necl3; (Maurel et al. 2007)), guinea pig polyclonal against Cadm3 (Necl1; (Maurel et al. 2007)) and chicken monoclonal against Cadm1 (Necl2, MBL CM004-3 at 1:1000). Recombinant EGF domain of human neuregulin-1-β1 (rhNrg1-EGFD) was from R&D Systems (396-HB) and 2.5S NGF was from AbD Serotec (PMP04Z).

Schwann cells, dorsal root ganglia (DRG) neurons, superior cervical ganglia (SCG) neurons, and myelinating co-cultures

The preparation of primary Schwann cells, DRG and SCG neurons, and myelinating cultures has been previously described (Kim and Maurel 2010). Briefly, Schwann cells were isolated from 2-day old rats and expanded in standard Schwann cell medium (DMEM, 1% GlutaMAX^{TM}-I, 10% heat-inactivated FBS) supplemented with 5 ng/ml of rhNrg1-EGFD and 2 μM Forskolin. In all experiments Schwann cells were used at the 4th passage. DRGs and SCGs were collected from embryonic day 15 rat embryos and 2-day-old rats, respectively. After trypsinization cells were plated on ø10mm glass coverslips coated with Matrigel, in standard neuronal medium (neurobasal medium, 2% B27 supplement, 1% GlutaMAX^{TM}-I, 0.08% glucose, and 50 ng/ml 2.5S NGF). DRG and SCG cells were seeded at a density of 1.3 and 0.8 ganglia per coverslip, respectively. Alternately feeding the cultures every 2 days with standard neuronal medium supplemented or not with 5-fluorodeoxyuridine and uridine (10 μM each) for 10 days removed non-neuronal cells. Purified neurons were then kept in standard neuronal medium until use. To establish co-cultures, purified neurons were repopulated with purified primary rat Schwann cells at a density of 200,000 cells per coverslip, in MEM supplemented with 10% heat inactivated FBS, 0.4% glucose and 50 ng/ml NGF. After 3 days, myelination was initiated by supplementing the media with 50 μg/ml of ascorbic acid. The formation of compact myelin segments was assessed by immunostaining for MBP, 10 days (DRG co-cultures) or 60 days (SCG co-cultures) later. To quantify the extent of myelination, 15 to 20 random fields were captured per culture (Nikon Eclipse TE2000-U, 20x/0.75 Plan Fluor objective). For each

condition, the average number of MBP-positive segments per field of view was calculated and normalized to that of the control cultures (100%). Counting was done with the ImageJ software (Schneider et al. 2012).

RNA interference of Cadm3 expression in DRG and SCG neurons

Two 21-nucleotide long shRNAs (#1, GGCCAGAAGCTGTTGTTACAT and #2, GTGCCAAGTGAAAGACCATGA) targeting in the extracellular domain of Cadm3 at position 733–753 and 911–931, respectively (GenBank NM_001047103), were designed using the following online tools: Easy siRNA (ProteinLounge), BLOCK-iT RNAi designer (Invitrogen) and siRNA sequence selector (Clontech). The shRNA stem loops consisted of a sense shRNA sequence followed by a short non-specific loop sequence (TTCAAGAGA) and the reverse/complement antisense shRNA sequence, followed by six thymidines that serve as a stop signal for the RNA polymerase III. The oligonucleotides were cloned into the HpaI-XhoI sites of the pLentiLox pLL3.7 lentiviral vector (Addgene, plasmid 11795), in which the U6 promoter drives the expression of the shRNA while the GFP marker is expressed under a CMV promoter (Dillon et al. 2005; Rubinson et al. 2003). The lentiviral constructs were transfected into 293FT cells together with packaging plasmids pMD2.G (Addgene plasmid 12259) and psPAX2 (Addgene plasmid 12260) using Lipofectamine 2000 (Invitrogen). We used a pLL3.7 construct encoding an shRNA against luciferase as a control for non-specific effects. Viral supernatants were collected 48 hrs after transfection, centrifuged at 1,600xg for 20 min to pellet cell debris, and supernatants were aliquoted for one-time use and kept frozen at −80ºC. For the infection, DRG or SCG cultures were treated with viral supernatants (supplemented with NGF at 50 ng/ml) 24hrs after plating the cells. The following day, alternate feeding to remove non-neuronal cells was initiated as described above. The knockdown of Cadm3 expression was confirmed by Western blotting before using the cultures.

Expression of Cadm3 in DRG neurons

The sequence encoding the influenza hemagglutin (HA) epitope was added by PCR to the amino-terminus of Cadm3 protein immediately after the signal peptide as predicted by the SignalP program (Nielsen et al. 1997). The cDNA encoding HA-Cadm3 was then inserted in the pLenti6/V5-D vector by directional TOPO cloning (Invitrogen) and the construct was confirmed by sequencing. The lentiviral construct was transfected into 293FT cells together with packaging plasmids pLP1, pLP2, and pLP/VSVG (Invitrogen) using Lipofectamine 2000. The pLenti6/V5 vector was used as control. Viral supernatant collection and infection of the DRG neurons was as described in the RNA interference section. Expression of HA-Cadm3 at the surface of axons was confirmed by live immunostaining for the HA tag, 10 days post infection, before use.

Immunostaining

DRG neurons, DRG-Schwann cell or SCG-Schwann cell cultures were rinsed in phosphate buffered saline (PBS) and fixed in 4% paraformaldehyde for 20 minutes. After washing with PBS, samples were permeabilized in ice-cold methanol for 20 minutes and incubated in blocking solution (5% normal donkey-serum, 0.3% Triton X100) for 1hr at room temperature. This was followed by an overnight incubation at 4°C with primary antibodies

against MBP and neurofilament M prepared in blocking solution. After washing with PBS, samples were incubated with secondary antibodies for 1hr. Nuclei of cells were visualized by staining with DAPI. Cultures were mounted in antifading agent Citifluor (Ted Pella). Preparations were examined by epifluorescence on a Nikon Eclipse TE2000-U (20x/0.75 objective) microscope. 15 to 20 random field images were acquired per culture using the MetaMorph software package (Molecular Devices). Quantitation was done in ImageJ.

Proliferation Assay

75,000 Schwann cells were plated onto dissociated DRG neuron cultures, in MEM supplemented with 10% heat inactivated FBS, 0.4% glucose and 50 ng/ml NGF. After 24 hr, cultures were fed with fresh media for another 24 hrs. Schwann cell proliferation was assessed using an EdU nuclear labeling assay. EdU (10 μM final concentration) was added during the last 4 hrs of culture, and was detected using the Clik-iT Alexa 488 kit according to the manufacturer's instructions (Life Technologies). Neurites were detected by immunostaining for neurofilament M and nuclei by DAPI. All cultures were mounted on glass slides in Citifluor and examined by epifluorescence microscopy. Images were acquired using the MetaMorph software package. EdU- and DAPI-labeled nuclei from 20 to 30 random fields per culture were counted. Three cultures per condition in three separate experiments were analyzed. Typically over 1000 cells were counted per condition. EdU incorporation was expressed as a percentage of Edu-labeled versus DAPI labeled nuclei.

Cadm3-Fc production, signaling pathways experiment and Western blot analysis

The cloning of Cadm3-Fc into the pcDNA3.1 TOPO vector (Invitrogen) and the production of the Cadm3-Fc fusion protein were previously described (Maurel et al. 2007). Schwann cells were plated at a density of 300,000 cells per well of a 24-well plate (Techno Plastic Products) coated with poly-L-lysine. The following day, cells were incubated for 3 hrs in defined media (DMEM/Ham's F12 (1/1), N2 supplement, 1% GlutaMAX^{TM}-I) to down regulate signaling pathways. Cells were then incubated for 30 minutes at room temperature with Cadm3-Fc at concentrations ranging from 0 to 20 nM. rhNrg1-EGFD (2.5 and 10 nM) was then added and cultures were incubated at 37°C for 10 min, at which time cell lysates were prepared in 25 mM Tris buffer pH 7.4, containing 95 mM NaCl, 1% SDS, protease and phosphatase inhibitors cocktails (Pierce). Lysates were boiled for 10 min and cleared by centrifugation at 16,000xg for 10 min. Protein concentrations were determined by the BCA method (Pierce). Ten micrograms of proteins were fractionated on 10% Bis/Tris polyacrylamide gels and transferred onto 0.2μm nitrocellulose membranes (Biorad). Appropriate regions of the blots were cut out and incubated with specific primary antibodies to probe for ErbB2, ErbB3, Akt, Erk1/2, Cadm3 and β-actin. After incubating with appropriate infrared secondary antibodies (LI-COR), protein bands were visualized and quantified with the Odyssey imaging system (LI-COR). For each signaling molecule analyzed, the ratio of phosphorylated versus total was first determined. Then for each Cadm3-Fc group, the background (0 nM of rhNrg1-EGF-D) was subtracted. Finally each value was normalized to the activation of the control (no Cadm3-Fc) at 10 nM of rhNrg1-EGFD (100%).

Co-immunoprecipitation analysis

$3x10^6$ Schwann cells were plated per ø100mm plates coated with poly-L-lysine, in standard Schwann cell medium supplemented with rhNrg1-EGFD and Forskolin. After 24hrs, cells were incubated for 3 hrs in defined media to down regulate signaling pathways, and then were further incubated for 30 minutes at room temperature with either Cadm3-Fc or human IgG (hu-IgG) at 20 nM. rhNrg-EGFD (10 nM) was then added and cultures incubated at 37°C for 10 min, at which time pathway stimulation was stopped by washing the cultures 3 times with ice-cold PBS. Proteins were extracted in 200 μl of a 1% NP-40 detergent solution prepared in 20 mM Tris, pH 7.4, 10% glycerol, 2.5 mM EGTA, 2.5 mM EDTA, protease and phosphatase inhibitors. Cell lysates were centrifuged (16,000xg for 15 min at 4°C) and protein concentrations of supernatants determined. For each condition (hu-IgG or Cadm3-Fc treated, plus or minus rhNrg1-EGFD stimulation), 300 μg of protein lysate was pre-cleared with 40 μl of agarose-conjugated goat anti-mouse beads (50% slurry; Sigma A6531) at 4°C for 30 min. Beads were then removed by a 15-sec centrifugation (16,000xg, 4°C) and pre-cleared lysates incubated overnight at 4°C with 1 μg of mouse anti ErbB3 antibody. ErbB3 was then immunoprecipitated with 40 μl of agarose-conjugated goat anti-mouse beads (50% slurry) for 90 min at 4°C. Beads were collected by a 15-sec centrifugation (16,000xg at 4°C), washed 3 times in 500 μl of lysis buffer, and boiled in Laemmli sample buffer for 5 min. Immunoprecipitated proteins were fractionated as described in the previous section. Appropriate regions of the blots were cut out and incubated with specific primary antibodies to probe for ErbB2, ErbB3, Cadm3-Fc, Cadm1, Cadm4 and PTPN13. After incubating with appropriate infrared secondary antibodies, protein bands were visualized with the Odyssey imaging system.

Neurite membrane preparation

Neurite membranes were prepared according to established protocols (Maurel and Salzer 2000; Salzer et al. 1980b; Taveggia et al. 2005). Briefly, purified DRG neuron cultures from 24-well plates (12 wells) were washed with ice-cold PBS, collected in a 1ml Dounce homogenizer (Kontes Co., Vineland, NJ) in 1 ml of ice-cold PBS, and homogenized with 30 strokes. The homogenate was centrifuged (80 g, 20 min, 4°C) to remove debris and collagen. The supernatant, diluted up to 7 ml, was then centrifuged at 35,000 g for 1 hr, at 4°C. The supernatant was discarded and the pellet was resuspended in ice-cold lysis buffer.

PCR for splice variants of Cadm3

TRIzol reagent (Invitrogen) was used for the extraction of total RNA from purified DRG neuron cultures. Total RNA was then used as template with the SuperScript III First-Strand Synthesis kit (Invitrogen) to produce cDNA from which specific targets were amplified by qRT-PCR performed on a LightCycler 480 II (Roche) using the Maxima SYBR green/ROX qPCR master mix (Thermo Scientific). Primers were designed using the online version 4.0.0 of Primer3web (Koressaar and Remm 2007; Untergasser et al. 2012). Sense primers were designed so that the last 5 bases overlapped exons 1-2 (X1 variant; 5'-ATCTTTCCCAGGACGGCTAC) or exons 1-3 (canonical variant, lacks exon 2; 5'-CAATCTTTCCCAGGACGATAGC) boundaries. Antisense primers were specific to exon 2 (5'-AGGGCTGGCTATCTTGACTG) or to exon 3 (5'-AGACCACTGCAGAGATGAGT).

Control primers were designed against HPRT1 (sense 5'-TGACACTGGTAAAACAATGCAGA in exon 6, and antisense 5'-ACTTCGAGAGGTCCTTTTCACC in exon 7). Melting point (Tm) curve analysis was done on all qRT-PCRs to verify the detection of a unique peak for each reaction, at the expected Tm. All endpoint reactions were separated on a 15% DNA polyacrylamide gel to confirm the detection of a unique amplicon of the expected size (Cadm3 canonical: 118bp; Cadm3 X1 variant: 129bp and HPRT1: 105bp)

Statistical Analysis

Myelination and proliferation data obtained were analyzed by one-way ANOVA followed by Bonferroni post-tests. Quantitative Western blots for Cadm2, Cadm3 and Nrg1 were analyzed by paired Student's t-test. The effects of Cadm3-Fc on the stimulation of pathways by rhNrg1-EGFD were analyzed by two-way ANOVA. Tests were performed with the Prism software package from GraphPad.

Results

Axonal Cadm3 is not necessary to promote Schwann cell myelination *in vitro*

To characterize the function of axonal Cadm3 in Schwann cell myelination, we created constructs expressing short-hairpin RNAs specific to Cadm3 and delivered them into DRG neurons by lentiviral infection. The viral constructs also encode for GFP, whose extensive expression in the neurite network of the infected DRG neurons demonstrates efficient transduction (Figure 1A). Both Cadm3 shRNAs that were tested effectively suppressed Cadm3 expression in DRG neurons, whereas a control shRNA directed against luciferase did not affect Cadm3 expression (Figure 1B). Immunostaining for neurofilament did not show any obvious defects in the formation of a dense neurite network by DRG neurons deficient in Cadm3, when compared to control (Figure 1A). We then tested the ability of Schwann cells to myelinate DRG neurons lacking Cadm3 at the surface of their neurites. Schwann cells myelinated equally well both control and shLuc-infected DRG neurons (Figure 1C–D). Cadm3-deficient neurites also efficiently supported the formation of compact myelin segments by Schwann cells. In fact a substantial and significant 3.5-fold increase in the number of myelin segments was observed (figure 1C–D). At 65±1 μm, the average myelin segment length was not statistically different from that of control (69±3 μm) and shLuc-infected DRG neurons (65±2 μm; p=0.485; one-way ANOVA; n = 4 experiments (ctrl, shLuc and shCadm3 #1); n = 3 experiments for shCadm3 #2; 3 cultures per condition, per experiment). These results suggest that Cadm3 expression on axons is not necessary to promote Schwann cell myelination. However they also suggest that axonal Cadm3 may be inhibitory to myelin formation.

Increased expression of axonal Cadm3 impairs Schwann cell myelination *in vitro*

To test the hypothesis that axonal expression of Cadm3 may be inhibitory to myelination, we used lentiviral infection of DRG neurons to deliver a cDNA construct that encoded for full length Cadm3 to which the hemaglutinin epitope (HA) was added at the N-terminus (Maurel et al. 2007). Live immunodetection of the HA tag indicated that Cadm3 was properly targeted at the surface of neurites (Figure 2A, top panels, red), and that the extent of the

neurite network was comparable to that of control DRG neuron cultures (Figure 2B, bottom panels, green). While Schwann cells formed numerous and comparable numbers of compact myelin segments around neurites from control DRG neurons (Figure 2B–C), there was a dramatic decrease (75%) in the numbers of myelin segments formed by Schwann cell in contact with DRG neurites expressing increased amounts of Cadm3 (Figure 2B–C). This result strongly suggests that indeed axonal Cadm3 may be inhibitory to myelination.

Superior cervical ganglion neurons are myelinated when deficient in axonal Cadm3

To further address a possible inhibitory role of Cadm3 in myelination, we compared by quantitative Western blotting the levels of Cadm3 expression between NGF-dependent peripheral neurons isolated from two different sources: the dorsal root ganglia (DRG) and the superior cervical ganglia (SCG). SCG neurons are sympathetic neurons whose axons are mostly ensheathed and unmyelinated *in vivo*. In co-culture with Schwann cells, SCG axons are also poorly ensheathed (Obremski et al. 1993) and remain largely unmyelinated. Interestingly we found that SCG neurons expressed about 2-fold more Cadm3 than DRG neurons did (Figure 3A, B). To account for a possible difference between DRG and SCG axons due to a different surface-to-volume ratio, data was normalized to either β-actin or TrkA, without any significant difference (Figure 3B). To test whether these high levels of Cadm3 expression may prevent Schwann cells to myelinate these normally unmyelinated axons, SCG neurons were infected with the lentiviral shRNA constructs that effectively suppressed expression of Cadm3. As with DRG neurons, neurite outgrowth was not impaired and an extensive network developed (Figure 3C; right panels). Rat Schwann cells were then added to control or Cadm3-deficient SCG cultures, and the resulting co-cultures maintained in myelinating media for 60 days. While few myelin segments were detected in control cultures, significant numbers of compact myelinated segments were visualized, by MBP staining, around axons deficient for Cadm3 (Figure 3C–D).

Axonal Cadm3 inhibits axon-mediated cell proliferation

To elucidate whether axonal Cadm3 was involved in regulating axon-mediated Schwann cell proliferation, we cultured Schwann cells onto the neurites of DRG neuron cultures that either normally expressed Cadm3, or that had been knocked-down with shRNA against Cadm3. Proliferation was assessed by the nuclear incorporation of Edu. As shown in Figure 4, the ablation of Cadm3 expression at the surface of DRG neurites resulted in a two-fold increase in the incorporation of Edu by Schwann cells. This result strongly indicates that contact-dependent stimulation of Schwann cell proliferation is regulated by the expression of Cadm3 at the surface of axons.

Type III Neuregulin-1 and Cadm2 expression is not affected by the presence or absence of Cadm3 in DRG neurons

DRG neurons regulate Schwann cell proliferation and myelination through several axon-derived factors (Pereira et al. 2012), in particular the type III isoform of Neuregulin-1 (Nrg1) (Michailov et al. 2004; Taveggia et al. 2005). We therefore performed quantitative Western blot analyses on lysates from neurite membrane preparations to determine possible changes in the expression of type III Nrg1 by DRG neurons in the absence of, or over-expression of Cadm3. As shown in Figure 5 changes in Cadm3 expression did not affect the expression of

type III Nrg1 significantly. We also analyzed for the expression of Cadm2, the only other identified cell adhesion ligand for Cadm4 to date (Maurel et al. 2007; Thomas et al. 2008). As for type III Nrg1, Cadm2 expression was not affected in DRG neurons knocked-down for, or over-expressing Cadm3 (Figure 5A, B).

Comparative levels of expression of Cadm3 *in vitro* and *in vivo*

Cadm3 levels are developmentally regulated *in vivo* (Figure 6C, p0 and p30 comparison), a finding that is in line with our previous *in vitro* data showing upregulation of Cadm3 upon axo-glial contact, in non-myelinating and myelinating conditions (Maurel et al. 2007). Since Cadm3 levels can potentially be regulated by context, we attempted to evaluate the relative amount of Cadm3 expression by DRG neurons *in vivo* and *in vitro.* Quantitation was done for the band at 43 kDa. The molecular weight corresponds to that calculated for the canonical form of Cadm3, it is DRG-specific (Figure 6A), and both the shCadm3 (Figure 1B) and the PCR for canonical Cadm3 (Figure 6B) confirm that it is Cadm3. PCR analysis failed to confirm the expression of a putative splice variant (X1; NCBI XM_006250323.2) with an expected MW of 47 kDa that has been predicted by automated computational analysis (NCBI annotation; (Kapustin et al. 2008)). Relative intensities of the 43 kDa band were measured by quantitative Western blots (Figure 6C, top panel) from purified DRG neurons, p0 and p30 sciatic nerve extracts, and normalized to relative intensities of neurofilament M (DRG marker). In sciatic nerves, Cadm3 expression is increased almost 8 fold from p0 to p30 (Figure 6C, bottom panel). The relative amount of Cadm3 in purified DRG neurons is about 50% that observed in p30 sciatic nerves (Figure 6C, bottom panel).

Cadm3 negatively regulate Neuregulin-1-mediated activation of ErbB3 and Akt

Key to Schwann cell proliferation and myelination is the activation of the PI3 kinase/Akt signaling cascade by Nrg1 (Maurel and Salzer 2000; Ogata et al. 2004). Another major pathway activated by Nrg1, with important implication to PNS myelination, is the Mek/Erk signaling cascade (He et al. 2010; Maurel and Salzer 2000; Newbern et al. 2011; Ogata et al. 2004; Syed et al. 2010). To determine whether Cadm3 interaction with Schwann cells could have an impact on the activation of these signaling pathways by Nrg-1, Schwann cells were first incubated for 30 minutes with Cadm3-Fc (0 to 20 nM), and then stimulated for 10 minutes with rhNrg1-EGFD (at 2.5 and 10 nM). Quantitative Western blotting (Figure 7) was used to determine the phosphorylated levels of Akt (S^{473}), Erk1/2 (Thr^{202}/Tyr^{204}), ErbB3 (Tyr^{1289}) and ErbB2 (Tyr^{1248}). In all conditions, ErbB2, ErbB3, Akt and Erk1/2 were significantly (Two-way ANOVA $p < 0.0001$) phosphorylated in a concentration-dependent manner by rhNRG1-EGFD treatment (Figure 7A–D). However the extent of activation of Akt and ErbB3 was dramatically and significantly ($p < 0.0001$) reduced (≈50%) by the presence of Cadm3-Fc (Figure 7A–B), in a concentration-dependent manner. Although there appeared to be an inhibitory trend on the Erk1/2 phosphorylation (≈30%; Figure 7C), it was not significant ($p = 0.1012$). ErbB2 phosphorylation on Tyr^{1248} was not affected as well (Figure 7D, $p = 0.8292$).

These experiments were designed to detect and measure the effect mediated on Schwann cells solely by the extracellular domain of Cadm3, independent of possible effects of Cadm3 levels on DRG axons, and demonstrate concentration-dependence, hence the use of Cadm3-

Fc. The Fc portion insures that the extracellular domain is presented as a *cis*-homodimer, similar to the normal assembly of full-length Cadm3 (Kakunaga et al. 2005). One caveats of course if that one cannot control the presentation of the Fc chimeric protein to the cells (*cis* or *trans*). The results are nonetheless informative as to the role of an interaction of the extracellular domain of Cadm3 with Schwann cells on signaling pathways activation, at concentrations (nM range) that are likely to be physiological. As to the EGF-like domain of neuregulin, it is necessary and sufficient to activate ErbB receptors and downstream signaling cascades (Buonanno and Fischbach 2001). Furthermore, within the time frame used in our experiments (10 min. treatment), the EGF-like domain of Nrg1 activates ErbB receptors with kinetics that are similar to that of full-length neuregulins (Syed and Kim 2010; Warren et al. 2006).

ErbB3 co-immunoprecipitates with Cadm3, but not with Cadm4 and Cadm1

The effect of the extracellular domain Cadm3 on ErbB3 and Akt activation suggested a possible interaction, direct or indirect, between Cadm3 and the ErbB receptors. To determine whether exogenous Cadm3 could be part of a complex with Schwann cell ErbB receptors, Schwann cells were first incubated for 30 minutes with Cadm3-Fc at 20 nM (human IgG at a similar concentration was used as a control), and then stimulated, or not, for 10 minutes with rhNrg1-EGFD at 10 nM. Schwann cells were then lysed, ErbB3 immunoprecipitated and the immunoprecipitated material analyzed by Western blotting (Figure 8). ErbB2 was co-immunoprecipitated with ErbB3 upon Nrg-1 stimulation (Figure 8), demonstrating effective recruitment of ErbB2 by ErbB3 upon ligand binding. There was no obvious difference between Schwann cells that had been treated with Cadm3-Fc or human IgG. Interestingly, Cadm3-Fc was also dramatically enriched in ErbB3 IP lanes, with or without rhNrg1-EGFD stimulation. As the human IgG was not co-IPed with ErbB3 in the control experiment, it is inferred that Cadm3-Fc co-immunoprecipitated with ErbB2/ErbB3 through an interaction, direct or indirect, that involves the extracellular domain, and not the Fc portion fused to it. The detection, in all ErbB3 IP lanes, of trace amounts of PTPN13 (a phosphatase that has been shown to down-regulate ErbB3 phosphorylation (Zhu et al. 2008), appears independent of Cadm3-Fc treatment and rhNrg1-EGFD stimulation. Cadm1 and Cadm4 (solid triangle), which have previously been shown to interact with ErbB3 (Kawano et al. 2009; Sugiyama et al. 2013), were not co-immunoprecipitated with ErbB3, regardless of the conditions. The band detected in the IP lane for Cadm4 (open triangle) corresponds to the heavy chain of the mouse anti-ErbB3 antibody used for the co-immunoprecipitation.

Discussion

In the present study we investigated the role of cell adhesion molecule Cadm3 during Schwann cell myelination. Cadm3 is expressed at the surface of the axons of DRG neurons (Maurel et al. 2007; Spiegel et al. 2007) while its heterophilic ligands Cadm1 and Cadm4 (Maurel et al. 2007; Thomas et al. 2008) are expressed by Schwann cells and are localized to the adaxonal membrane that is in close apposition with the axon (Maurel et al. 2007; Spiegel et al. 2007). Therefore the Cadms are thought to promote axo-glial interactions through Cadm3/Cadm1 and Cadm3/Cadm4 associations. The detachment of the adaxonal membrane away from the axon that is observed in the Cadm4 knockout mouse supports that view

(Golan et al. 2013). In addition the delayed onset of myelination observed in this knockout mouse (Golan et al. 2013) is also in agreement with *in vitro* studies that showed that Schwann cells whose Cadm4 function has been abolished or perturbed fail to progress to the pro-myelinating stage (Maurel et al. 2007) and are stopped at the one-full-turn association with an axon, failing to spiral wrap further to form compact myelin sheathes (Spiegel et al. 2007).

Considering the strong heterophilic interaction exhibited between Cadm3 and Cadm4 (Maurel et al. 2007; Thomas et al. 2008), it is interesting that the analysis of two independent Cadm3 knockout mice (Golan et al. 2013; Park et al. 2008) did not reveal any phenotypes affecting myelination in the PNS. These results may suggest that either 1) Cadm3 is dispensable for PNS myelination, 2) compensatory mechanisms are involved, 3) Cadm3 does not provide the pro-myelinating function as Cadm4 does, or 4) Cadm3 provides different regulatory mechanisms – pro-myelinating or inhibitory – depending on its binding partners on Schwann cells. It is also possible that the time frame of the *in vivo* analyses (7 days (Park et al. 2008) to 60 days (Golan et al. 2013; Park et al. 2008)) does not overlap with the time frame of Cadm3 function or observable phenotype. For example, the E-cadherin knockout mouse has a delayed onset of myelination observable at post-natal day p2 that is recovered from by post-natal day p14 (Basak et al. 2015).

We therefore turned to an *in vitro* approach to determine a possible role for Cadm3 that was not revealed by the *in vivo* approach. We used the long-established Schwann cell/DRG myelinating co-culture system (Bunge et al. 1967) that has been central to the identification of key molecules and processes governing axo-glial interactions, domain formation and PNS myelination (Dzhashiashvili et al. 2007; Eldridge et al. 1989; Eshed et al. 2005; Maurel et al. 2007; Maurel and Salzer 2000; Melendez-Vasquez et al. 2004; Salzer et al. 1980a; Spiegel et al. 2007; Taveggia et al. 2005). We show strong evidence that Cadm3 may provide an inhibitory regulatory mechanism to Schwann cell myelination. Ablation of Cadm3 expression from DRG neurons results in a striking increase in the number of myelinated segments (Figure 1C–D). Conversely, the over-expression of Cadm3 on the axonal surface of DRG neurons results in an almost complete inability by Schwann cells to form myelin segments (Figure 2B–C).

An increase in Edu incorporation, suggestive of increased Schwann cell proliferation, was also observed concomitant with increased myelination (Figure 4). Since exit from the cell cycle is a pre-requisite to differentiation, it is unlikely that the effect of axonal Cadm3 on Schwann cell myelination can be attributed to a regulation of the cell cycle. The effect of axonal Cadm3 could then be a simple consequence of an increase in Schwann cell numbers resulting in an increase in myelin segments, and *vice-versa*. However the result obtained with SCG neurons whose axons do not support myelination, both *in vivo* and *in vitro* (Brunden et al. 1992; Obremski et al. 1993; Roufa et al. 1986), precludes that possibility. We found that NGF-dependent SCG neurons express much higher levels of Cadm3 compared to NGF-dependent DRG neurons (Figure 3A–B) and, most strikingly, decreasing these levels induced the formation of a significant number of myelin segments (Figure 3C–D). NGF-dependent SCG and DRG neurons in purified cultures, i.e. in the absence of Schwann cells, have neurites of similar diameter (Estridge and Bunge 1978; Windebank et al. 1985).

However to account for a possible difference in surface-to-volume ratio between both type of neurons in the cultures, Cadm3 relative intensities were normalized to either actin (axoplasm) or TrkA (axonal plasma membrane). Cadm3 levels were similarly higher in SCG lysates, 1.7 vs 1.8, actin vs TrkA, respectively (Figure 3A–B). This suggests that the difference in expression of Cadm3 between SCG and DRG neurons is not dependent on differences in surface-to-volume ratio, and may represent differences in transcriptional, post-transcriptional and/or translational controls between myelinated and non-myelinated fibers. These results therefore suggest that the amount of Cadm3 expressed at the surface of axons is sufficient to alter the fate of the Schwann cells in contact with these axons. In particular it suggests that, at least *in vitro*, high levels of axonal Cadm3 are inhibitory to Schwann cell myelin formation whereas low levels would be permissive.

In that respect it is interesting to note the significant decrease in Cadm3 expression in the 4.1B knockout mouse (Einheber et al. 2013) which exhibits an about 3-fold increase in the number of small caliber axons (1 μm) being myelinated in the sciatic nerve (Einheber et al. 2013), as well as a slight, but significant, hyper-myelination across all axon diameters (Cifuentes-Diaz et al. 2011; Einheber et al. 2013). This is of course an indirect correlation, and it is quite possible that the phenotype observed in the 4.1B knockout mice is not related to the decrease in axon-derived Cadm3. However, along with the *in vitro* data, it does shed lights on the apparent lack of phenotype in the PNS of the Cadm3 knockout mouse (Golan et al. 2013; Park et al. 2008). Indeed one would predict a hypermyelinating phenotype in the Cadm3$^{-/-}$ mouse. A major difference between the 4.1$^{-/-}$ and the Cadm3$^{-/-}$ mice is the time frame at which EM analyses were done: 4 to 13 months (4.1B$^{-/-}$) and 7 days to 2 months (Cadm3$^{-/-}$). While the difference in g-ratio, in 4.1B$^{-/-}$ mice, was small at 4 and 6 months, it was reported to increase in mice growing older (13 months, (Cifuentes-Diaz et al. 2011)). It is therefore possible that an overall difference in g-ratio may not have been detectable in 2-month old Cadm3 knockout mice, but could be in older mice. In addition a detailed analysis of the number of myelinated axons, binned per axon diameter, may reveal an increase in the number of small caliber axons being myelinated, as was shown in the 4.1B$^{-/-}$ mice (Einheber et al. 2013). Of course one cannot preclude a possible role for Cadm3 also at the onset of myelination that, when knocked-out, may produce a transient phenotype no longer observable at p7 (earliest time point of the Cadm3$^{-/-}$ analysis; (Park et al. 2008)). Observation at time points earlier that post-natal p7 may reveal phenotypes such as a higher number of axons sorted out in 1:1 relationship or a decreased g-ratio in the Cadm3$^{-/-}$ mice. Since the Cadm3$^{-/-}$ mice generated by Park et al. (2008) and Golan et al. (2013) are pan knockouts, an analysis of the SCG sympathetic track to detect myelinated fibers would also be informative.

To assess whether the *in vitro* inhibitory effect of Cadm3 may be relevant *in vivo*, we attempted to evaluate if Cadm3 expression by purified DRG neurons *in vitro* was within physiological levels. The quantitative analysis shown in Figure 6C indicates that while Cadm3 levels in DRG are higher than that of p0 sciatic nerve extracts, they are 50% lower than that of p30 nerve extracts. It is important to keep in mind that this comparison is quite relative, since the *in vivo* levels are underestimated due to presence of Schwann cells and fibroblasts, as well as to the large increased expression in myelin proteins. It is also not possible to determine cell type contribution. The results however suggest that Cadm3 *in vitro*

levels are likely to be within bounds of *in vivo* levels and that the *in vitro* results on myelination may therefore be physiologically relevant. An *in vivo* determination of the relative amount of Cadm3 on axons of similar calibers, myelinated versus non-myelinated, as determined by electron microscopy (EM), would be informative. The current Cadm3 antibodies however are not suitable for EM studies.

The lack of phenotype in the Cadm3$^{-/-}$ mice, as well as the increase in myelination in the culture system after abolishing Cadm3 expression, could also result from the expression of another cell adhesion molecule compensating for the loss of Cadm3. A possible candidate is Cadm2, which, as far as we know, is the only other known ligand for Cadm4 (Maurel et al. 2007; Thomas et al. 2008). Our results (Figure 5) however show that Cadm2 expression by DRG neurons, at least *in vitro*, is not affected by the absence or over-expression of Cadm3. In addition, we have previously shown that Cadm4 fails to bind to DRG neurons that are deficient in Cadm3. This further underscores the lack of significant amount and upregulation of Cadm2, as well as other potential compensatory ligand for Cadm4, in Cadm3-deficient DRG neurons (Maurel et al. 2007).

If one considers the negative impact of axonal Cadm3 on both Schwann cell proliferation and myelination, the data suggest that Cadm3 may interfere with a pathway that is common to both biological outcomes. On the axon, type III Nrg1 is the key molecule regulating Schwann cell proliferation and myelination (Michailov et al. 2004; Taveggia et al. 2005), through the activation of the PI3 kinase/Akt signaling cascade (Domènech-Estevez et al. 2016; Maurel and Salzer 2000; Ogata et al. 2004). Therefore two possibilities come to mind. i) Cadm3 affects type III Nrg1 expression and/or plasma membrane presence, which however does not appear to be the case since type III Nrg1 levels are not significantly changed in neurite preparations from Cadm1 knockdown and over-expressing DRG neurons (Figure 5). Or ii) Cadm3 affects activation of the ErbB receptors. Consistent with this latter possibility is our finding that the extracellular domain of Cadm3 significantly inhibits the rhNrg1-EGFD–mediated activation of ErbB3 on Tyr^{1289}, a docking site for the p85 subunit of PI3 kinase (Schulze et al. 2005)), and that of downstream PI3 kinase effecter Akt (Figure 7A–B). Interestingly, this inhibitory effect is specific to the PI3 kinase/Akt pathway insofar that the activation of the MEK/Erk1/2 pathway by Nrg1 is not particularly affected by Cadm3 (Figure 7C). This is corroborated by the lack of effect on ErbB2 phosphorylation on Tyr^{1248} (Figure 7D), which couples ErbB2 to the Ras/Raf/Erk signaling cascade (Ben-Levy et al. 1994; Kwon et al. 1997; Muthuswamy et al. 1999).

These results suggest that the extracellular domain of Cadm3 decoupled the Akt and Erk intracellular pathways that were activated by rhNrg1-EGFD and the ErbB2/ErbB3 receptors. A similar finding has been described with Herstatin, which uncouples the Akt and Erk pathways that are activated by EGF and the EGF receptor (EGFR, (Justman and Clinton 2002)). The specific mechanism(s) that impart this apparent specificity to Cadm3 on Nrg1-activated pathways is (are) unclear. Although it does not appear to be the mode of action for Herstatin (Justman and Clinton 2002), one possible mechanism is that the extracellular domain of Cadm3 affects the apparent concentration of, or alters the binding affinity of the EGF domain of Nrg1 to ErbB3. An alternative is that, as with Herstatin (Azios et al. 2001; Justman and Clinton 2002), Cadm3 prevents heterodimerization of ErbB2 and ErbB3 upon

ligand binding to ErbB3. Our coIP experiments however, done in conditions of maximum activation of the Akt and Erk pathways (10 nM of rhNrg1-EGFD; see Figure 7), suggest that the extracellular domain of Cadm3 does not impair ErbB2/ErbB3 interaction upon rhNrg1-EGFD binding, since no noticeable differences in the coIP of ErbB2 with ErbB3 were observed between Cadm3-Fc and hu-IgG conditions (Figure 8). This finding also suggests that extracellular domain of Cadm3 does not affect the binding of rhNrg1-EGFD to ErbB3 since the stabilization of the interaction between ErbB2 and ErbB3 results from a change in conformation that is mediated upon ligand binding to ErbB3 (Citri and Yarden 2006). These data are in agreement with that of Kawano et al. (2009) whose results also suggest that the interaction of Cadm1 with ErbB3 does not prevent ligand binding to ErbB3 and recruitment of ErbB2. Even in the event of a disruption of ErbB2/ErbB3 dimerization, it would be difficult to draw a definitive conclusion. Indeed, while Herstatin has been shown to prevent dimerization of the EGF receptor, along with a decrease in overall EGFR phosphorylation (Azios et al. 2001; Justman and Clinton 2002), only the Akt pathway was affected, without any effect on the Erk pathway. This result strongly suggests that Herstatin binding to the EGFR probably affected the EGFR pattern of phosphorylation, leaving the docking site for Grb2 (involved in Erk pathway activation (Ravichandran 2001)) unaltered. Interestingly it is what we observed with Cadm3 (Figure 7), a specific decrease in phosphorylation of Tyr^{1289} on ErbB3 (docking site for the p85 subunit of PI3 kinase (Schulze et al. 2005)), while the specific site for activation of the Erk pathway, Tyr^{1248} on ErbB2, was unaffected. A similar differential phosphorylation resulting in differential signaling has been described for ErbB4, albeit induced by different Nrg1 ligands (Sweeney et al. 2000). One mechanism that would alter ErbB phosphorylation profile and impact phospho-tyrosine docking site usage is the recruitment to ErbB complexes of specific regulatory components. For example, phosphatases such as Ptprz and PTPN13 have been shown to repress the phosphorylation of ErbB2 (Scrima et al. 2012; Zhu et al. 2008), ErbB3 (Kawano et al. 2009; Sugiyama et al. 2013) and ErbB4 (Fujikawa et al. 2007). Interestingly, PTPN13 was recently shown to interact with Cadm1 and Cadm4 (Kawano et al. 2009; Sugiyama et al. 2013), ligands for axonal Cadm3 that are both present on Schwann cells (Maurel et al. 2007; Spiegel et al. 2007; Thomas et al. 2008). Cadm1 and Cadm4 were also shown to interact with ErbB3 through their extracellular domains (Kawano et al. 2009; Sugiyama et al. 2013). This interaction does not prevent ErbB2 recruitment upon ligand binding to ErbB3 (Kawano et al. 2009). We did detect PTPN13 in our ErbB3 coIP experiments (Figure 8), and this pull-down was not affected by the presence of Cadm3-Fc. As mentioned earlier, ErbB2 was also coIPed, confirming that PTPN13 is present in ErbB2/ErbB3 complexes. As anticipated we also coIPed Cadm3-Fc. Surprisingly however, neither Cadm1 nor Cadm4 were detected, which raises the question on how both Cadm3 and PTPN13 are associated with ErbB2/ErbB3 in Schwann cells. Since Cadm1 and Cadm4 were not detected in the control IP (non specific human IgG in place of Cadm3-Fc; Figure 8), it is unlikely that Cadm3-Fc displaced their interaction with ErbB3. Either both Cadm1 and Cadm4 do not interact significantly with ErbB receptors in an endogenous setting (compared to ectopic over-expression for the reported interactions), or interactions were disrupted during the coIP process. While that latter possibility cannot be ruled out, it is unlikely since the antibody used for the coIP recognizes an intracellular epitope on ErbB3, and ErbB2 and Cadm3-Fc coIP (extracellular

interactions) were not prevented. PTPN13 contains five PDZ domains, and it being coIPed in absence of Cadm1 and Cadm4, suggests that additional components may be involved.

To summarize, our *in vitro* studies strongly support a function for Cadm3 in PNS myelination. While the molecular regulatory mechanisms are not clearly understood, the extracellular domain of Cadm3 has the potential to interfere with the activation of the ErbB3/PI3K/Akt signaling cascade, which is the pro-myelinating pathway in the PNS. Interestingly the Erk1/2 pathway, which has inhibitory properties (Harrisingh et al. 2004; Ogata et al. 2004; Parkinson et al. 2008; Syed et al. 2010; Yang et al. 2012), was unaffected. The selective inhibitory effect of Cadm3 may represent a regulatory mechanism that help Schwann cells integrate the neuregulin signal to switch between different biological outcomes such as proliferation, survival, ensheathment and myelination. There remains to determine the relevance of these finding to *in vivo* myelination, since analyses of Cadm3$^{-/-}$ mice have not detected any phenotypes. The lack of phenotype is not however contradictory in itself. Since Cadm3 is dramatically upregulated at post-natal day 30, when the process of active myelination is over, Cadm3 may not provide an inhibitory mechanism at the onset of myelination, but later on during myelin maintenance. An analysis of the Cadm3 knockout mice at older age, as was done on the 4.1B$^{-/-}$ mice, may be informative.

Acknowledgments

We would like to thank Drs James L. Salzer, Steven Einheber and Haesun Kim for helpful discussion. This work was supported by grants to P.M. from the NIH/NINDS (R01 NS065218) and the Charles and Johanna Busch Memorial Fund at Rutgers, The State University of New Jersey. The content is solely the responsibility of the authors and does not necessarily represent the official views of the National Institute Of Neurological Disorders And Stroke (NINDS) or the National Institutes of Health (NIH).

Abbreviations

Cadm	cell adhesion molecule
CNS	central nervous system
DRG	dorsal root ganglia
EGF	epidermal growth factor
EGFR	epidermal growth factor receptor
EM	electron microscopy
ErbB	erythroblastic leukemia viral oncogene homolog
GFAP	glial fibrillary acidic protein
GFP	green fluorescent protein
HPRT1	Hypoxanthine Phosphoribosyltransferase 1
MBP	myelin basic protein
Mpz	myelin protein zero

Necl	nectin-like
NFM	neurofilament medium chain
NGF	nerve growth factor
Nrg1	neuregulin-1
PBS	phosphate buffer saline
PNS	peripheral nervous system
rhNrg1-EGFD	recombinant human EGF- like domain of Nrg1-β1
shRNA	small hairpin ribonucleic acid
SynCAM	synaptic cell adhesion molecule
TrkA	Tropomyosin receptor kinase A

References

Azios NG, Romero FJ, Denton MC, Doherty JK, Clinton GM. Expression of herstatin, an autoinhibitor of HER-2/neu, inhibits transactivation of HER-3 by HER-2 and blocks EGF activation of the EGF receptor. Oncogene. 2001; 20(37):5199–209. [PubMed: 11526509]

Basak S, Desai DJ, Rho EH, Ramos R, Maurel P, Kim HA. E-cadherin enhances neuregulin signaling and promotes Schwann cell myelination. Glia. 2015; 63(9):1522–36. [PubMed: 25988855]

Ben-Levy R, Paterson HF, Marshall CJ, Yarden Y. A single autophosphorylation site confers oncogenicity to the Neu/ErbB-2 receptor and enables coupling to the MAP kinase pathway. EMBO J. 1994; 13(14):3302–11. [PubMed: 7913890]

Biederer T. Bioinformatic characterization of the SynCAM family of immunoglobulin-like domain-containing adhesion molecules. Genomics. 2006; 87(1):139–50. [PubMed: 16311015]

Brunden KR, Ding Y, Hennington BS. Myelin protein expression in dissociated superior cervical ganglia and dorsal root ganglia cultures. J Neurosci Res. 1992; 32(4):507–15. [PubMed: 1527797]

Bunge MB, Bunge RP, Peterson ER, Murray MR. A light and electron microscope study of long-term organized cultures of rat dorsal root ganglia. J Cell Biol. 1967; 32(2):439–66. [PubMed: 10976233]

Buonanno A, Fischbach GD. Neuregulin and ErbB receptor signaling pathways in the nervous system. Curr Opin Neurobiol. 2001; 11(3):287–96. [PubMed: 11399426]

Cifuentes-Diaz C, Chareyre F, Garcia M, Devaux J, Carnaud M, Levasseur G, Niwa-Kawakita M, Harroch S, Girault JA, Giovannini M, et al. Protein 4.1B contributes to the organization of peripheral myelinated axons. PLoS One. 2011; 6(9):e25043. [PubMed: 21966409]

Citri A, Yarden Y. EGF-ERBB signalling: towards the systems level. Nat Rev Mol Cell Biol. 2006; 7(7):505–16. [PubMed: 16829981]

Clary DO, Weskamp G, Austin LR, Reichardt LF. TrkA cross-linking mimics neuronal responses to nerve growth factor. Mol Biol Cell. 1994; 5(5):549–63. [PubMed: 7919537]

Cotter L, Ozcelik M, Jacob C, Pereira JA, Locher V, Baumann R, Relvas JB, Suter U, Tricaud N. Dlg1-PTEN interaction regulates myelin thickness to prevent damaging peripheral nerve overmyelination. Science. 2010; 328(5984):1415–8. [PubMed: 20448149]

Dillon CP, Sandy P, Nencioni A, Kissler S, Rubinson DA, Van Parijs L. Rnai as an experimental and therapeutic tool to study and regulate physiological and disease processes. Annu Rev Physiol. 2005; 67:147–73. [PubMed: 15709955]

Domènech-Estevez E, Baloui H, Meng X, Zhang Y, Deinhardt K, Dupree JL, Einheber S, Chrast R, Salzer JL. Akt Regulates Axon Wrapping and Myelin Sheath Thickness in the PNS. J Neurosci. 2016; 36(16):4506–21. [PubMed: 27098694]

Dzhashiashvili Y, Zhang Y, Galinska J, Lam I, Grumet M, Salzer JL. Nodes of Ranvier and axon initial segments are ankyrin G-dependent domains that assemble by distinct mechanisms. J Cell Biol. 2007; 177(5):857–70. [PubMed: 17548513]

Einheber S, Meng X, Rubin M, Lam I, Mohandas N, An X, Shrager P, Kissil J, Maurel P, Salzer JL. The 4.1B cytoskeletal protein regulates the domain organization and sheath thickness of myelinated axons. Glia. 2013; 61(2):240–53. [PubMed: 23109359]

Eldridge CF, Bunge MB, Bunge RP. Differentiation of axon-related Schwann cells in vitro: II. Control of myelin formation by basal lamina. J Neurosci. 1989; 9(2):625–38. [PubMed: 2918381]

Eshed Y, Feinberg K, Poliak S, Sabanay H, Sarig-Nadir O, Spiegel I, Bermingham JR Jr, Peles E. Gliomedin mediates Schwann cell-axon interaction and the molecular assembly of the nodes of Ranvier. Neuron. 2005; 47(2):215–29. [PubMed: 16039564]

Estridge M, Bunge R. Compositional analysis of growing axons from rat sympathetic neurons. J Cell Biol. 1978; 79(1):138–55. [PubMed: 151689]

Fujikawa A, Chow JP, Shimizu H, Fukada M, Suzuki R, Noda M. Tyrosine phosphorylation of ErbB4 is enhanced by PSD95 and repressed by protein tyrosine phosphatase receptor type Z. J Biochem. 2007; 142(3):343–50. [PubMed: 17646177]

Garratt AN, Britsch S, Birchmeier C. Neuregulin, a factor with many functions in the life of a schwann cell. Bioessays. 2000; 22(11):987–96. [PubMed: 11056475]

Goebbels S, Oltrogge JH, Wolfer S, Wieser GL, Nientiedt T, Pieper A, Ruhwedel T, Groszer M, Sereda MW, Nave KA. Genetic disruption of Pten in a novel mouse model of tomaculous neuropathy. EMBO Mol Med. 2012; 4(6):486–99. [PubMed: 22488882]

Golan N, Kartvelishvily E, Spiegel I, Salomon D, Sabanay H, Rechav K, Vainshtein A, Frechter S, Maik-Rachline G, Eshed-Eisenbach Y, et al. Genetic deletion of Cadm4 results in myelin abnormalities resembling Charcot-Marie-Tooth neuropathy. J Neurosci. 2013; 33(27):10950–61. [PubMed: 23825401]

Harrisingh MC, Perez-Nadales E, Parkinson DB, Malcolm DS, Mudge AW, Lloyd AC. The Ras/Raf/ERK signalling pathway drives Schwann cell dedifferentiation. EMBO J. 2004; 23(15): 3061–71. [PubMed: 15241478]

He Y, Kim JY, Dupree J, Tewari A, Melendez-Vasquez C, Svaren J, Casaccia P. Yy1 as a molecular link between neuregulin and transcriptional modulation of peripheral myelination. Nat Neurosci. 2010; 13(12):1472–80. [PubMed: 21057508]

Justman QA, Clinton GM. Herstatin, an autoinhibitor of the human epidermal growth factor receptor 2 tyrosine kinase, modulates epidermal growth factor signaling pathways resulting in growth arrest. J Biol Chem. 2002; 277(23):20618–24. [PubMed: 11934884]

Kakunaga S, Ikeda W, Itoh S, Deguchi-Tawarada M, Ohtsuka T, Mizoguchi A, Takai Y. Nectin-like molecule-1/TSLL1/SynCAM3: a neural tissue-specific immunoglobulin-like cell-cell adhesion molecule localizing at non-junctional contact sites of presynaptic nerve terminals, axons and glia cell processes. J Cell Sci. 2005; 118(Pt 6):1267–77. [PubMed: 15741237]

Kao SC, Wu H, Xie J, Chang CP, Ranish JA, Graef IA, Crabtree GR. Calcineurin/NFAT signaling is required for neuregulin-regulated Schwann cell differentiation. Science. 2009; 323(5914):651–4. [PubMed: 19179536]

Kapustin Y, Souvorov A, Tatusova T, Lipman D. Splign: algorithms for computing spliced alignments with identification of paralogs. Biol Direct. 2008; 3:20. [PubMed: 18495041]

Kawano S, Ikeda W, Kishimoto M, Ogita H, Takai Y. Silencing of ErbB3/ErbB2 signaling by immunoglobulin-like Necl-2. J Biol Chem. 2009; 284(35):23793–805. [PubMed: 19561085]

Kim, HA.; Maurel, P. Primary Schwann Cell Culture. In: Doering, LC., editor. Protocols for Neural Cell Culture. Humana Press; 2010. p. 253-268.

Koressaar T, Remm M. Enhancements and modifications of primer design program Primer3. Bioinformatics. 2007; 23(10):1289–91. [PubMed: 17379693]

Kwon YK, Bhattacharyya A, Alberta JA, Giannobile WV, Cheon K, Stiles CD, Pomeroy SL. Activation of ErbB2 during wallerian degeneration of sciatic nerve. J Neurosci. 1997; 17(21): 8293–9. [PubMed: 9334404]

Maurel P, Einheber S, Galinska J, Thaker P, Lam I, Rubin MB, Scherer SS, Murakami Y, Gutmann DH, Salzer JL. Nectin-like proteins mediate axon Schwann cell interactions along the internode and are essential for myelination. J Cell Biol. 2007; 178(5):861–74. [PubMed: 17724124]

Maurel P, Salzer JL. Axonal regulation of Schwann cell proliferation and survival and the initial events of myelination requires PI 3-kinase activity. J Neurosci. 2000; 20(12):4635–45. [PubMed: 10844033]

Melendez-Vasquez CV, Einheber S, Salzer JL. Rho kinase regulates schwann cell myelination and formation of associated axonal domains. J Neurosci. 2004; 24(16):3953–63. [PubMed: 15102911]

Meyer D, Yamaai T, Garratt A, Riethmacher-Sonnenberg E, Kane D, Theill LE, Birchmeier C. Isoform-specific expression and function of neuregulin. Development. 1997; 124(18):3575–86. [PubMed: 9342050]

Michailov GV, Sereda MW, Brinkmann BG, Fischer TM, Haug B, Birchmeier C, Role L, Lai C, Schwab MH, Nave KA. Axonal neuregulin-1 regulates myelin sheath thickness. Science. 2004; 304(5671):700–3. [PubMed: 15044753]

Muthuswamy SK, Gilman M, Brugge JS. Controlled dimerization of ErbB receptors provides evidence for differential signaling by homo- and heterodimers. Mol Cell Biol. 1999; 19(10):6845–57. [PubMed: 10490623]

Newbern JM, Li X, Shoemaker SE, Zhou J, Zhong J, Wu Y, Bonder D, Hollenback S, Coppola G, Geschwind DH, et al. Specific functions for ERK/MAPK signaling during PNS development. Neuron. 2011; 69(1):91–105. [PubMed: 21220101]

Nielsen H, Engelbrecht J, Brunak S, von Heijne G. A neural network method for identification of prokaryotic and eukaryotic signal peptides and prediction of their cleavage sites. Int J Neural Syst. 1997; 8(5–6):581–99. [PubMed: 10065837]

Obremski VJ, Johnson MI, Bunge MB. Fibroblasts are required for Schwann cell basal lamina deposition and ensheathment of unmyelinated sympathetic neurites in culture. J Neurocytol. 1993; 22(2):102–17. [PubMed: 8445407]

Ogata T, Iijima S, Hoshikawa S, Miura T, Yamamoto S, Oda H, Nakamura K, Tanaka S. Opposing extracellular signal-regulated kinase and Akt pathways control Schwann cell myelination. J Neurosci. 2004; 24(30):6724–32. [PubMed: 15282275]

Park J, Liu B, Chen T, Li H, Hu X, Gao J, Zhu Y, Zhu Q, Qiang B, Yuan J, et al. Disruption of Nectin-like 1 cell adhesion molecule leads to delayed axonal myelination in the CNS. J Neurosci. 2008; 28(48):12815–9. [PubMed: 19036974]

Parkinson DB, Bhaskaran A, Arthur-Farraj P, Noon LA, Woodhoo A, Lloyd AC, Feltri ML, Wrabetz L, Behrens A, Mirsky R, et al. c-Jun is a negative regulator of myelination. J Cell Biol. 2008; 181(4):625–37. [PubMed: 18490512]

Pellissier F, Gerber A, Bauer C, Ballivet M, Ossipow V. The adhesion molecule Necl-3/SynCAM-2 localizes to myelinated axons, binds to oligodendrocytes and promotes cell adhesion. BMC Neurosci. 2007; 8:90. [PubMed: 17967169]

Pereira JA, Lebrun-Julien F, Suter U. Molecular mechanisms regulating myelination in the peripheral nervous system. Trends Neurosci. 2012; 35(2):123–34. [PubMed: 22192173]

Ravichandran KS. Signaling via Shc family adapter proteins. Oncogene. 2001; 20(44):6322–30. [PubMed: 11607835]

Roufa D, Bunge MB, Johnson MI, Cornbrooks CJ. Variation in content and function of non-neuronal cells in the outgrowth of sympathetic ganglia from embryos of differing age. J Neurosci. 1986; 6(3):790–802. [PubMed: 3514817]

Rubinson DA, Dillon CP, Kwiatkowski AV, Sievers C, Yang L, Kopinja J, Rooney DL, Zhang M, Ihrig MM, McManus MT, et al. A lentivirus-based system to functionally silence genes in primary mammalian cells, stem cells and transgenic mice by RNA interference. Nat Genet. 2003; 33(3): 401–6. [PubMed: 12590264]

Salzer JL, Brophy PJ, Peles E. Molecular domains of myelinated axons in the peripheral nervous system. Glia. 2008; 56(14):1532–40. [PubMed: 18803321]

Salzer JL, Bunge RP, Glaser L. Studies of Schwann cell proliferation. III. Evidence for the surface localization of the neurite mitogen. J Cell Biol. 1980a; 84(3):767–78. [PubMed: 6153659]

Salzer JL, Williams AK, Glaser L, Bunge RP. Studies of Schwann cell proliferation. II. Characterization of the stimulation and specificity of the response to a neurite membrane fraction. J Cell Biol. 1980b; 84(3):753–66. [PubMed: 7358797]

Schneider CA, Rasband WS, Eliceiri KW. NIH Image to ImageJ: 25 years of image analysis. Nat Methods. 2012; 9(7):671–5. [PubMed: 22930834]

Schulze WX, Deng L, Mann M. Phosphotyrosine interactome of the ErbB-receptor kinase family. Mol Syst Biol. 2005; 1:2005–0008.

Scrima M, De Marco C, De Vita F, Fabiani F, Franco R, Pirozzi G, Rocco G, Malanga D, Viglietto G. The nonreceptor-type tyrosine phosphatase PTPN13 is a tumor suppressor gene in non-small cell lung cancer. Am J Pathol. 2012; 180(3):1202–14. [PubMed: 22245727]

Spiegel I, Adamsky K, Eshed Y, Milo R, Sabanay H, Sarig-Nadir O, Horresh I, Scherer SS, Rasband MN, Peles E. A central role for Necl4 (SynCAM4) in Schwann cell-axon interaction and myelination. Nat Neurosci. 2007; 10(7):861–9. [PubMed: 17558405]

Sugiyama H, Mizutani K, Kurita S, Okimoto N, Shimono Y, Takai Y. Interaction of Necl-4/CADM4 with ErbB3 and integrin alpha6 beta4 and inhibition of ErbB2/ErbB3 signaling and hemidesmosome disassembly. Genes Cells. 2013; 18(6):519–28. [PubMed: 23611113]

Sweeney C, Lai C, Riese DJ 2nd, Diamonti AJ, Cantley LC, Carraway KL 3rd. Ligand discrimination in signaling through an ErbB4 receptor homodimer. J Biol Chem. 2000; 275(26):19803–7. [PubMed: 10867024]

Syed N, Kim HA. Soluble Neuregulin and Schwann Cell Myelination: a Therapeutic Potential for Improving Remyelination of Adult Axons. Mol Cell Pharmacol. 2010; 2(4):161–167. [PubMed: 21274416]

Syed N, Reddy K, Yang DP, Taveggia C, Salzer JL, Maurel P, Kim HA. Soluble neuregulin-1 has bifunctional, concentration-dependent effects on Schwann cell myelination. J Neurosci. 2010; 30(17):6122–31. [PubMed: 20427670]

Takai Y, Miyoshi J, Ikeda W, Ogita H. Nectins and nectin-like molecules: roles in contact inhibition of cell movement and proliferation. Nat Rev Mol Cell Biol. 2008; 9(8):603–15. [PubMed: 18648374]

Taveggia C, Zanazzi G, Petrylak A, Yano H, Rosenbluth J, Einheber S, Xu X, Esper RM, Loeb JA, Shrager P, et al. Neuregulin-1 type III determines the ensheathment fate of axons. Neuron. 2005; 47(5):681–94. [PubMed: 16129398]

Thomas LA, Akins MR, Biederer T. Expression and adhesion profiles of SynCAM molecules indicate distinct neuronal functions. J Comp Neurol. 2008; 510(1):47–67. [PubMed: 18615557]

Untergasser A, Cutcutache I, Koressaar T, Ye J, Faircloth BC, Remm M, Rozen SG. Primer3--new capabilities and interfaces. Nucleic Acids Res. 2012; 40(15):e115. [PubMed: 22730293]

Warren CM, Kani K, Landgraf R. The N-terminal domains of neuregulin 1 confer signal attenuation. J Biol Chem. 2006; 281(37):27306–16. [PubMed: 16825199]

Windebank AJ, Wood P, Bunge RP, Dyck PJ. Myelination determines the caliber of dorsal root ganglion neurons in culture. J Neurosci. 1985; 5(6):1563–9. [PubMed: 4009246]

Wolpowitz D, Mason TB, Dietrich P, Mendelsohn M, Talmage DA, Role LW. Cysteine-rich domain isoforms of the neuregulin-1 gene are required for maintenance of peripheral synapses. Neuron. 2000; 25(1):79–91. [PubMed: 10707974]

Yang DP, Kim J, Syed N, Tung YJ, Bhaskaran A, Mindos T, Mirsky R, Jessen KR, Maurel P, Parkinson DB, et al. p38 MAPK activation promotes denervated Schwann cell phenotype and functions as a negative regulator of Schwann cell differentiation and myelination. J Neurosci. 2012; 32(21):7158–68. [PubMed: 22623660]

Zhu JH, Chen R, Yi W, Cantin GT, Fearns C, Yang Y, Yates JR 3rd, Lee JD. Protein tyrosine phosphatase PTPN13 negatively regulates Her2/ErbB2 malignant signaling. Oncogene. 2008; 27(18):2525–31. [PubMed: 17982484]

Main points

Cadm3 is a cell adhesion molecule that promotes axo-glial interactions in the PNS. Increasing levels of axonal Cadm3 inhibit Schwann cell myelination in vitro. The extracellular domain of Cadm3 negatively affects the ErbB3/PI3K/Akt pathway.

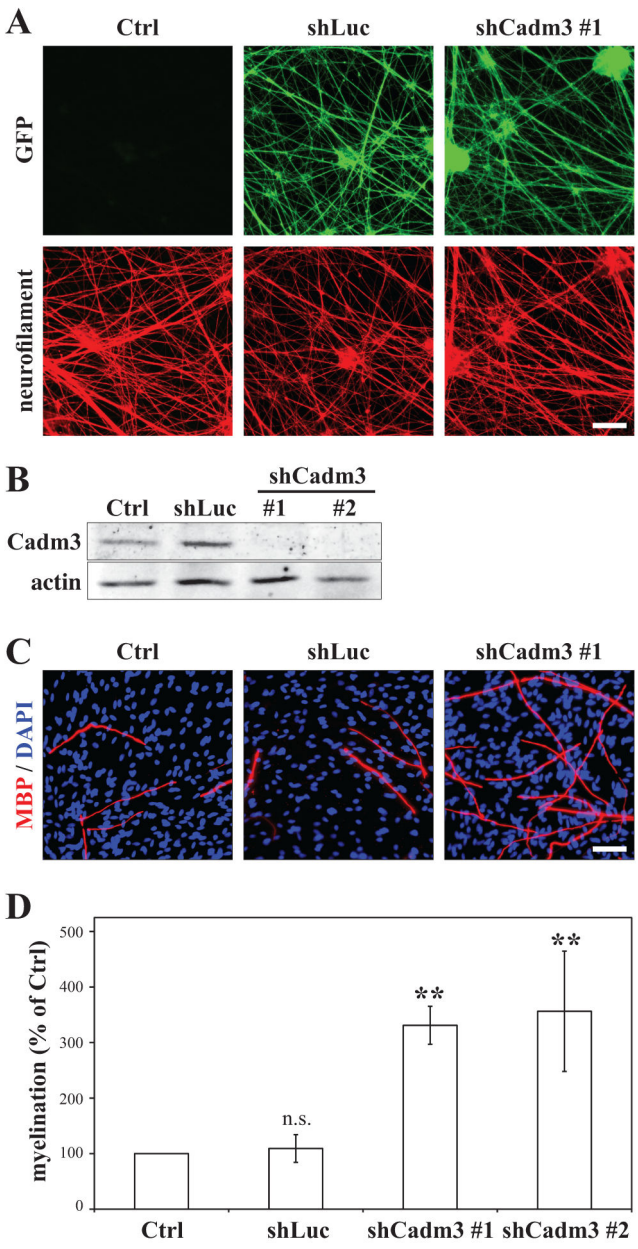

Figure 1. Axonal Cadm3 is not necessary for the myelination of DRG axons by Schwann cells in a myelinating co-culture system

DRG neurons were infected with lentiviruses encoding either an shRNA to a non-specific sequence (shLuc), or shRNAs (shCadm3 #1 and #2) specific to Cadm3. (A) Constructs expressed GFP, whose detection by immunostaining in the neurite network demonstrates efficient tranduction. Controls (Ctrl) are non-infected cultures. All cultures were co-immunostained for neurofilament (red). Scale bar = 50 μm. (B) Western blot analysis of DRG neuron cultures demonstrating the effective knockdown of Cadm3 expression (shCadm3 #1 and #2) in DRG neurons. Non-infected DRG neurons (ctrl) and DRG neurons infected with the shLuc lentivirus serve as controls. (C) Representative images of myelinating co-cultures established with Schwann cells added to control DRG neurons (Ctrl,

shLuc) or to DRG neurons knocked-down for Cadm3 expression (shCadm3 #1). Myelin segments were detected by immunostaining for myelin basic protein (MBP, red); Schwann cell nuclei were labeled with DAPI (blue). Scale bar = 50 μm. (D) Quantitation of the effect of Cadm3 knockdown (shCadm3 #1, #2) in DRG neurons on Schwann cell myelination. Controls are non-infected (Ctrl) and shLuc-infected DRG neurons. Mean ± SEM from n = 4 (Ctrl, shLuc, shCadm3 #1) and n = 3 (shCadm3 #2) independent experiments. One-way ANOVA ($p = 0.0018$) followed by Bonferroni post-hoc analysis (n.s. = not significant; ** $p<0.01$).

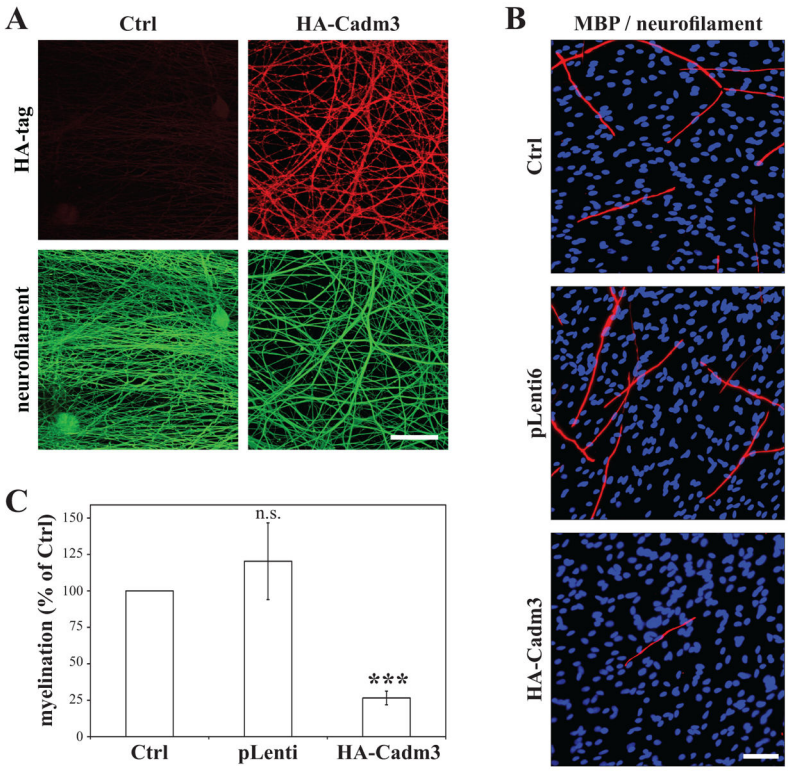

Figure 2. Increased expression of axonal Cadm3 impairs myelination by Schwann cells in a myelinating co-culture system

(A) DRG neurons were infected with a lentivirus driving the expression of Cadm3 (HA-Cadm3) at the surface of axons, as shown by live immuno-detection of the HA tag (red). (B) Representative images of myelinating co-cultures established with Schwann cells added to control DRG neurons (Ctrl = non-infected; pLenti = infected with a construct expressing GFP), or to neurons over-expressing Cadm3 (HA-Cadm3). Myelin segments were immunostained for MBP (red); Schwann cell nuclei were labeled with DAPI (blue). Scale bar = 50 μm. (C) Quantitation of the effect of Cadm3 over-expression in DRG neurons on Schwann cell myelination. Controls are non-infected (Ctrl) and pLenti-infected DRG neurons. Mean ± SEM from n = 4 independent experiments. One-way ANOVA ($p = 0.0036$) followed by Bonferroni post-hoc analysis (n.s. = not significant; *** $p<0.001$).

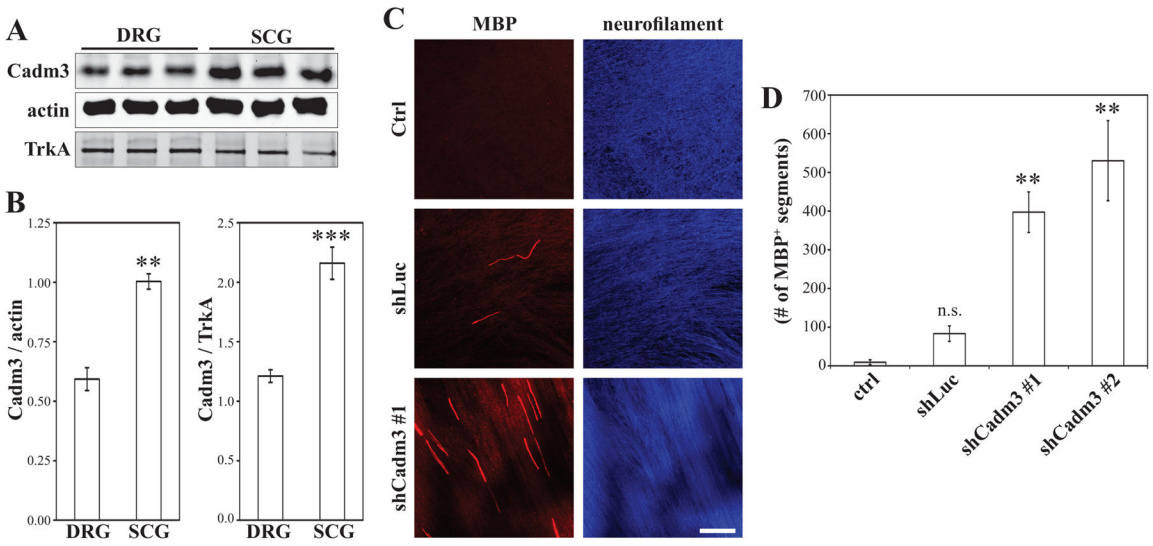

Figure 3. SCG neurons are myelinated in the absence of Cadm3

(A) Lysates of NGF-dependent DRG, and NGF-dependent SCG neurons (three independent lysates, respectively) were fractionated by Western blotting and quantitatively analyzed (B). While both types of neurons express Cadm3, the levels of expression are about 2-fold higher in SCG neurons. Student's t-test (** p = 0.0019; *** p = 0.0004). (C) Schwann cells form myelin segments (MBP immunostained red) when associated with SCG neurons that were first infected with shRNA lentiviruses against Cadm3 (shCadm3 #1). Controls were non-infected SCG neurons (Ctrl), and SCG neurons infected with the non-specific shLuc construct. (D) Quantitation of the number of myelinating segments. Mean ± SEM from n = 3 independent experiments. One-way ANOVA (p = 0.0008 followed by Bonferroni post-hoc analysis (n.s. = not significant; ** p<0.01).

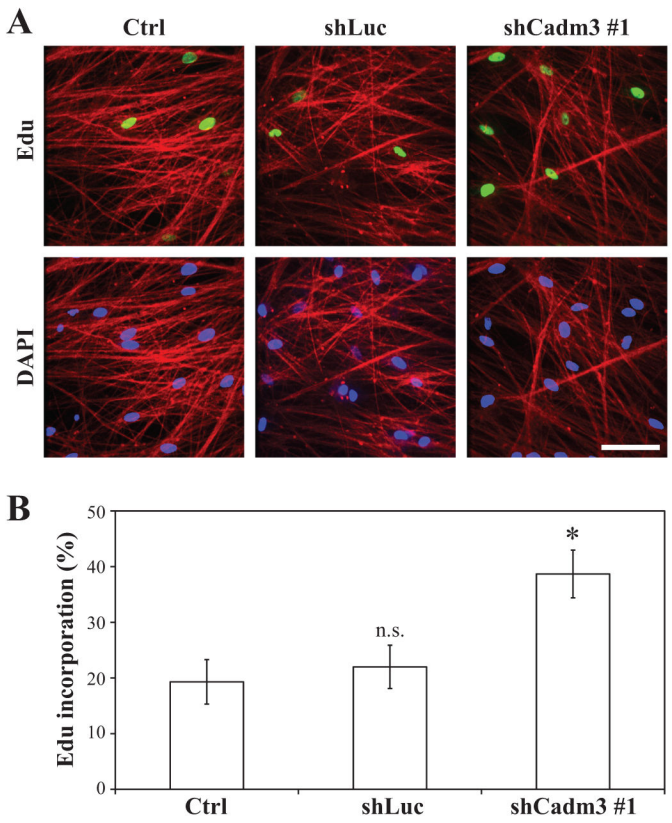

Figure 4. Knockdown of Cadm3 expression in DRG neurons promotes axon-mediated Schwann cell proliferation

(A) Schwann cells were seeded onto control DRG neurons (Ctrl, shLuc) or DRG neurons knocked-down for Cadm3 expression (shCadm3 #1). After 24hrs, the co-cultures were treated with Edu and Schwann cell proliferation was assessed by immunostaining for incorporated Edu (green). (B) Quantitation of Edu incorporation as a % of Edu-positive nuclei among DAPI-stained nuclei. Values represent the mean ± SEM from n = 3 independent experiments. One-way ANOVA ($p = 0.0316$) followed by Bonferroni post-hoc analysis (n.s. = not significant; *, $p<0.05$).

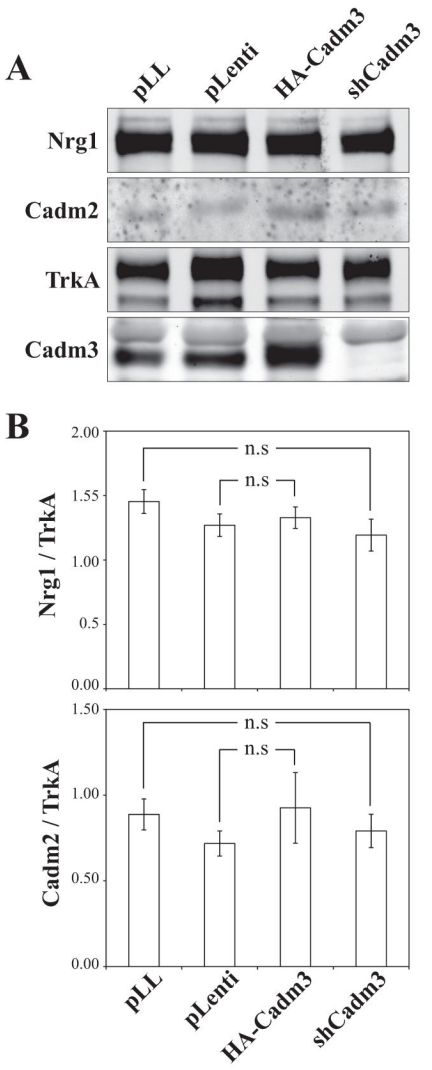

Figure 5. Cadm3 levels do no affect expression of Type III Neuregulin-1 and Cadm2 on neurites of DRG neurons

Neurite membranes, prepared from control DRG neurons (pLL, plenti) or DRG neurons knockdown for (shCadm3) or over-expressing (HA-Cadm3) Cadm3, were analyzed by quantitative Western blotting for the expression of type III Nrg1 and Cadm2, a ligand for Schwann cell Cadm4. pLL is the vector control for the shRNA data, whereas plenti is the vector control for the over-expression data. Data was normalized using TrkA as a neurite membrane marker. No significant changes were observed. Values represent the mean ± SEM from n = 3 independent experiments. Student's t-test (n.s. = not significant).

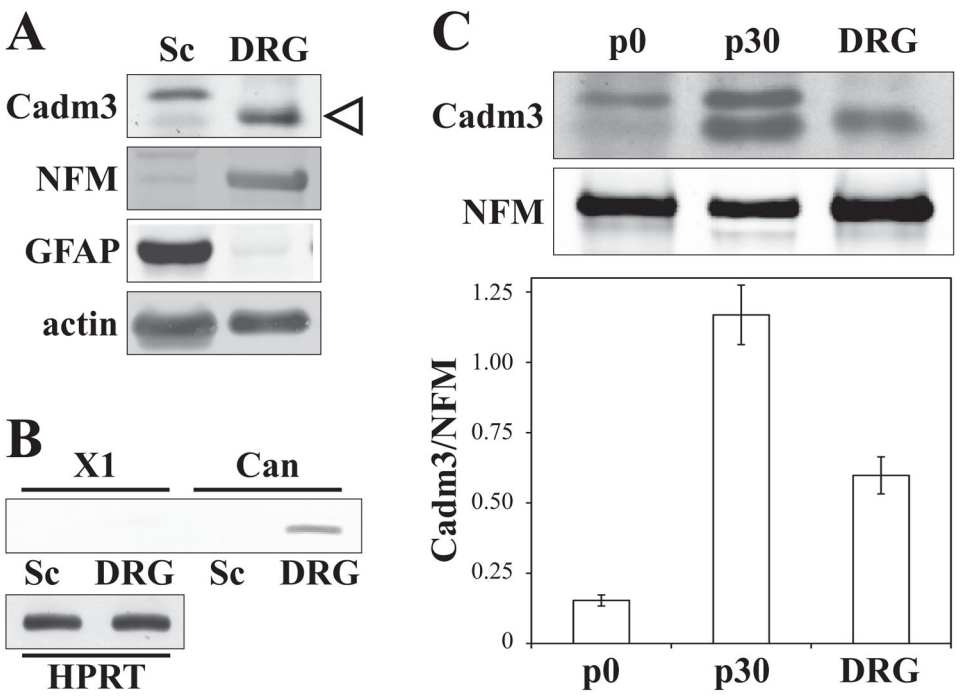

Figure 6. Comparative assessment of Cadm3 expression *in vitro* and *in vivo*

Lysates of Schwann cells (Sc), DRG neurons (DRG), post-natal day 0 (p0, birth) and day 30 (p30) sciatic nerves were qualitatively (panel A) and quantitatively (panel C) analyzed for the expression of Cadm3. Two bands were detected at 43 kDa (lower band indicated by open triangle) and 47 kDa. Neurofilament (NFM) and GFAP were used as DRG neuron and Schwann cell specific markers, respectively. PCR analysis (panel B), done on DRG and Schwann cell cDNA, detected a specific 118bp product for the canonical (Can), 43 kDa Cadm3, in DRG neurons only. No band (129bp) for a computationally predicted 47 kDa splice variant (X1) was detected in Schwann cells. HPRT1 is used as control. The 43 kDa was used for the quantitation shown in panel C, normalized to NFM. Values represent the mean ± SEM from n = 3 independent experiments.

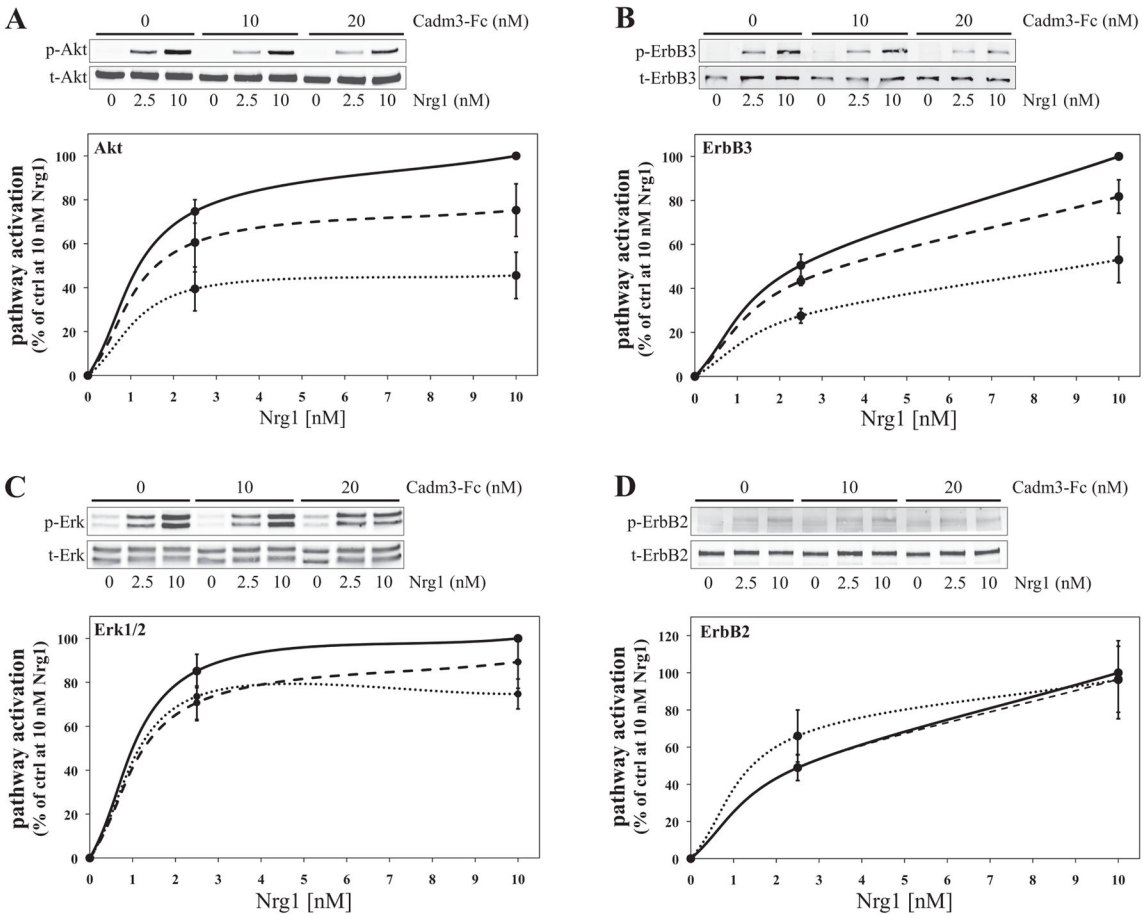

Figure 7. Cadm3 inhibits Nrg1-mediated activation of ErbB3 and Akt in Schwann cells

Schwann cells were first maintained in defined media for 24hrs and then incubated with Cadm3-Fc at various concentrations (0 nM = solid line; 10 nM = dash line; 20 nM = dotted line) for 30 min., before stimulation with rhNrg1-EGFD (Nrg1; 0, 2.5 and 10 nM). Phosphorylated and total levels of Akt, ErbB3, Erk and ErbB2 (blots A, B, C and D, respectively) were analyzed by quantitative Western blotting. Mean ± SEM from n = 4 (ErbB2, ErbB3) and n=7 (Akt, Erk1/2) independent experiments. In all Cadm3-Fc conditions, rhNrg1-EGFD stimulated the activation of ErbB2, ErbB3, Akt and Erk1/2 (Two-way ANOVA, $p < 0.0001$). However increasing concentrations of Cadm3-Fc do significantly reduce by about 50% the effect of rhNrg1-EGFD stimulation (Two-way ANOVA, $p < 0.0001$). Cadm3-Fc has no inhibitory effect on the activation of ErbB2 (Two-way ANOVA, $p = 0.1012$) and Erk1/2 (Two-way ANOVA, $p = 0.8292$).

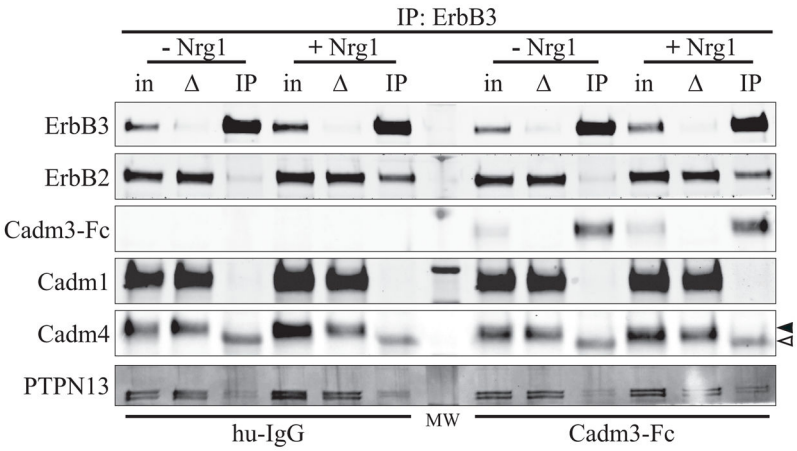

Figure 8. ErbB3 and ErbB2 co-immunoprecipitates with Cadm3

Schwann cells were first maintained in defined media for 24hrs and then incubated with Cadm3-Fc (20 nM) for 30 min., before stimulation with rhNrg1-EGFD (Nrg1; 10 nM). Human IgG (hu-IgG) is used as a control for the specificity of the Cadm3-Fc interaction. ErbB3 immunoprecipitated complexes were then analyzed for the presence of ErbB2, Cadm3-Fc, Cadm1, Cadm4, and PTPN13. For each condition, three lanes were run: “in” represents the input lanes (2% of material use for IP), “Δ” represents the depleted material after IP (2% of material used for IP, after the IP), and “IP” represents the immunoprecipitated lanes. The solid triangle indicates Cadm4, whereas the open triangle corresponds to the heavy chain of the mouse anti-ErbB3 antibody used for the co-immunoprecipitation.